Study of Frequency Characteristics for Three-Coil Wireless Power Transfer System with Different Positions

Xueyi Zhang[1], Yang Yuan[1], and Zhongqi Li[1, 2, *]

Abstract—To explore the problem that the frequency characteristics of a magnetically coupled three-coil wireless power transfer (WPT) system are affected with different positions, in this paper, the expressions of the resonant frequency and the frequency corresponding to the maximum output power are deduced based on equivalent circuit theory. It is concluded that not only the resonant frequency is changed with different positions, but also the frequency corresponding to the maximum output power is changed with different positions. The WPT system always features a maximum efficiency point and a maximum output power point. The frequencies of the two points are almost the same. Finally, a three-coil experiment setup is built, and experimental results are well consistent with calculation and simulation results, which verifies the correctness of the proposed method. Proposed method provides a feasible scheme for simultaneously achieving high efficiency and high output power, and also provides a useful reference for the further research on the frequency tracking and optimization control algorithms.

1. INTRODUCTION

In recent years, the traditional wired power supply system has been unable to satisfy people's requirements for mobility and special occasions because mobile devices develop rapidly, and there are some outstanding problems (such as electric spark and non-smart power supply) in the traditional wired power supply system. Therefore, wireless power transfer (WPT) technology has become a research hotspot [1–4]. In 2007, Kurs et al. in Massachusetts Institute of Technology proposed a magnetically coupled resonant WPT system, which was called WiTricity technology [5]. This technology can not only achieve mid-range wireless power transfer, but also be insensitive to the direction of the transmission device and receiving device [6, 7]. At present, many scholars have studied this technology [8–11]. It is found that the resonant frequency of a magnetically coupled resonant WPT system is a core parameter that determines the performance of the system [12, 13]. The efficiency of a WPT system is maximized when the system works in a resonant state. However, in practical applications, the system will inevitably be disturbed by the external environment, which results in frequency drift. The efficiency of the system will be greatly reduced when the frequency drift occurs [14–16]. Therefore, the research on the frequency characteristics of a WPT system has important practical significance for the improvement of the WPT system performance.

In [17], a two-coil WPT system with different resonant frequencies is modeled and analyzed. The efficiency is proved to peak at the resonant frequency of the receiving circuit, regardless of the resonant frequency of the transmission circuit. Using this feature, selective power transmission can be achieved by setting the receiving circuits at different resonant frequencies. Reference [18] proposes the optimum resonant frequency of transmission coil (Tx) driven by a series-resonant inverter in a WPT system. It

is found that if the resonant frequency of Tx is too close to the switching frequency of the inverter, the efficiency of the WPT system is reduced.

The frequency characteristics of a magnetically coupled resonant two-coil WPT system are analyzed by the above references. However, the efficiency of the two-coil WPT system will be deteriorated when the transmission distance is increased. When a relay coil is added between the transmission coil and the receiving coil, the working performance of the system will be greatly improved [19]. Compared to a two-coil WPT system, the transmission distance is longer, and the transmission efficiency is higher with a three-coil WPT system [20]. For the frequency characteristics of a three-coil WPT system, [21, 22] have studied the frequency splitting phenomenon of a three-coil WPT system and the change of the resonant frequency caused by the non-adjacent coupling between the transmission coil and the receiving coil. However, to the best of our knowledge, the effect of different positions on the resonant frequency and the frequency corresponding to the maximum output power of the WPT system is rarely studied.

In order to solve the above problem, the expressions of the resonant frequency, transmission efficiency, and output power of the three-coil WPT system are deduced. The effect of frequency characteristics on WPT system performance is studied with the help of MATLAB. In addition, a set of experimental devices is designed. The correctness of calculated and simulated results is verified by experimental results. The research conclusions provide a feasible scheme for simultaneously achieving high efficiency and output power.

2. MATHEMATICAL MODEL WITH DIFFERENT POSITIONS

The three-coil magnetically coupled resonant WPT system is shown in Figure 1, which consists of an AC source power, a transmission coil (Tx), a relay coil (Ix), a receiving coil (Rx), and a load. Parameter C_1 is the resonant capacitance of the transmission coil. Parameter C_2 is the resonant capacitance of the relay coil. Parameter C_3 is the resonant capacitance of the receiving coil. Parameter d_1 is the vertical distance between the transmission coil and relay coil. Parameter d_2 is the vertical distance between the relay coil and receiving coil. Parameter Δ_1 is the horizontal distance between the transmission coil and relay coil. Parameter Δ_2 is the horizontal distance between the relay coil and receiving coil. Parameter Δ_3 is the horizontal distance between the transmission coil and receiving coil.
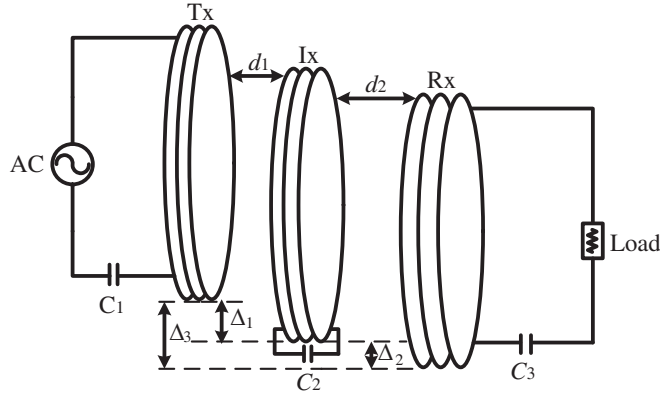
Figure 1. Diagram of three-coil WPT system.

As shown in Figure 2, the three-coil WPT system can be represented in terms of lumped circuit elements (L, C, and R). Parameter V_s denotes the AC voltage source, R_1 the internal resistance of the Tx, R_2 the internal resistance of the Ix, R_3 the internal resistance of the Rx, R_s the internal resistance of the voltage source, and R_L the load resistance. Parameter L_1 is the self-inductance of Tx, L_2 the self-inductance of Ix, L_3 the self-inductance of Rx, M_{12} the mutual inductance between Tx and Ix, M_{13} the mutual inductance between Tx and Rx, and M_{23} the mutual inductance between Ix and Rx. Variable Z_{in} is the input impedance of the three-coil WPT system, ω_0 the original resonant frequency, and ω the operating resonant frequency of the three-coil WPT system.
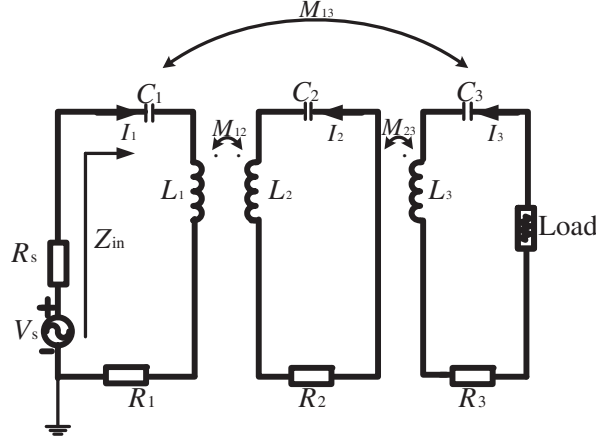
Figure 2. Equivalent circuit diagram of three-coil WPT system.

According to the Kirchhoff's voltage law, the three-coil WPT system model can be expressed as:

$$Z_1 \dot{I_1} + j\omega M_{12} \dot{I_2} + j\omega M_{13} \dot{I_3} = \dot{V_s}$$
$$j\omega M_{12} \dot{I_1} + Z_2 \dot{I_2} + j\omega M_{23} \dot{I_3} = 0 \tag{1}$$
$$j\omega M_{13} \dot{I_1} + j\omega M_{23} \dot{I_2} + Z_3 \dot{I_3} = 0$$

$$Z_1 = R_s + R_1 + j\omega L_1 + 1/(j\omega C_1)$$
$$Z_2 = R_2 + j\omega L_2 + 1/(j\omega C_2) \tag{2}$$
$$Z_3 = R_L + R_3 + j\omega L_3 + 1/(j\omega C_3)$$

where $\dot{I_1}$, $\dot{I_2}$, and $\dot{I_3}$ are the currents of the Tx, Ix, and Rx, respectively.

According to Eqs. (1) and (2), the expressions of $\dot{I_1}$, $\dot{I_2}$, and $\dot{I_3}$ can be obtained as follows:

$$\dot{I_1} = \frac{Z_2 Z_3 + (\omega M_{23})^2}{Z_1 Z_2 Z_3 + (\omega M_{23})^2 Z_1 + (\omega M_{13})^2 Z_2 + (\omega M_{12})^2 Z_3 - j2\omega^3 M_{12} M_{13} M_{23}} \dot{V_s} \tag{3}$$

$$\dot{I_2} = -\frac{\omega^2 M_{13} M_{23} + j\omega M_{12} Z_3}{Z_1 Z_2 Z_3 + (\omega M_{23})^2 Z_1 + (\omega M_{13})^2 Z_2 + (\omega M_{12})^2 Z_3 - j2\omega^3 M_{12} M_{13} M_{23}} \dot{V_s} \tag{4}$$

$$\dot{I_3} = -\frac{\omega^2 M_{12} M_{23} + j\omega M_{13} Z_2}{Z_1 Z_2 Z_3 + (\omega M_{23})^2 Z_1 + (\omega M_{13})^2 Z_2 + (\omega M_{12})^2 Z_3 - j2\omega^3 M_{12} M_{13} M_{23}} \dot{V_s} \tag{5}$$

According to Eqs. (3), (4), and (5), the efficiency and output power of the WPT system can be expressed as follows:

$$\eta = \left| \frac{\dot{I_3^2} R_L}{\dot{V_s} \dot{I_1}} \right| = \left| \frac{\left(\omega^2 M_{12} M_{23} + j\omega M_{13} Z_2 \right)^2 R_L}{\left[Z_2 Z_3 + (\omega M_{23})^2 \right]^2 [Z_1 Z_2 Z_3 + (\omega M_{23})^2 Z_1 + (\omega M_{13})^2 Z_2 + (\omega M_{12})^2 Z_3 - j2\omega^3 M_{12} M_{13} M_{23}]} \right| \tag{6}$$

$$P_{\text{out}} = \left| \dot{I_3^2} R_L \right| = \left| \left[\frac{\omega^2 M_{12} M_{23} + j\omega M_{13} Z_2}{Z_1 Z_2 Z_3 + (\omega M_{23})^2 Z_1 + (\omega M_{13})^2 Z_2 + (\omega M_{12})^2 Z_3 - j2\omega^3 M_{12} M_{13} M_{23}} V_s \right]^2 R_L \right| \tag{7}$$

By differentiating P_{out} with respect to ω and equating the differential function to zero,

$$\frac{\partial P_{\text{out}}}{\partial \omega} = 0 \tag{8}$$

According to Eq. (8), the frequency corresponding to the maximum output power can be obtained with the help of MATLAB.

The expression of the input impedance is defined as follows:

$$Z_{\text{in}} = V_{\text{s}}/I_1 - R_{\text{s}} \tag{9}$$

According to Eq. (9), the expression of the input impedance angle can be obtained as follows:

$$\theta = \arctan[\text{Im}(Z_{\text{in}})/\text{Re}(Z_{\text{in}})] \tag{10}$$

where $\text{Re}(Z_{\text{in}})$ denotes the real part of Z_{in}, and $\text{Im}(Z_{\text{in}})$ denotes the image part of Z_{in}. Let Eq. (10) equal zero ($\theta = 0$), Eq. (11) can be obtained as follows:

$$A\omega^{11} + B\omega^9 + C\omega^7 + D\omega^5 + E\omega^3 + F\omega = 0 \tag{11}$$

where

$$
\begin{aligned}
A = {}&(C_1C_2C_3M_{23}^2 - C_1C_2C_3L_2L_3)(C_1C_2C_3L_2M_{13}^2 + C_1C_2C_3L_3M_{12}^2 \\
&+C_1C_2C_3L_1M_{23}^2 - C_1C_2C_3L_1L_2L_3 - 2C_1C_2C_3M_{12}M_{13}M_{23}),
\end{aligned}
$$

$$
\begin{aligned}
B = {}&((C_1C_2L_2 + C_1C_3L_3)(C_1C_2C_3L_2M_{13}^2 + C_1C_2C_3L_3M_{12}^2 + C_1C_2C_3L_1M_{23}^2 - C_1C_2C_3L_1L_2L_3 \\
&-2C_1C_2C_3M_{12}M_{13}M_{23}) - C_1C_2C_3L_2R_{\text{L}}(C_1C_2C_3M_{12}^2R_{\text{L}} + C_1C_2C_3M_{23}^2R_{\text{s}} - C_1C_2C_3L_1L_2R_{\text{L}} \\
&-C_1C_2C_3L_2L_3R_{\text{s}}) + (C_1C_2C_3M_{23}^2 - C_1C_2C_3L_2L_3)(C_1C_2L_1L_2 - C_1C_3M_{13}^2 - C_2C_3M_{23}^2 \\
&-C_1C_2M_{12}^2 + C_1C_3L_1L_3 + C_2C_3L_2L_3 + C_1C_2C_3L_2R_{\text{L}}R_{\text{s}})),
\end{aligned}
$$

$$
\begin{aligned}
C = {}&((C_1C_2L_2 + C_1C_3L_3)(C_1C_2L_1L_2 - C_1C_3M_{13}^2 - C_2C_3M_{23}^2 - C_1C_2M_{12}^2 + C_1C_3L_1L_3 + C_2C_3L_2L_3 \\
&+C_1C_2C_3L_2R_{\text{L}}R_{\text{s}}) - C_1C_2C_3L_2R_{\text{L}}(C_1C_3L_1R_{\text{L}} + C_2C_3L_2R_{\text{L}} + C_1C_2L_2R_{\text{s}} + C_1C_3L_3R_{\text{s}}) \\
&-C_1(C_1C_2C_3L_2M_{13}^2 + C_1C_2C_3L_3M_{12}^2 + C_1C_2C_3L_1M_{23}^2 - C_1C_2C_3L_1L_2L_3 - 2C_1C_2C_3M_{12}M_{13}M_{23}) \\
&-(C_1C_2C_3M_{23}^2 - C_1C_2C_3L_2L_3)(C_1L_1 + C_2L_2 + C_3L_3 + C_1C_3R_{\text{L}}R_{\text{s}}) + C_1C_3R_L(C_1C_2C_3M_{12}^2R_{\text{L}} \\
&+C_1C_2C_3M_{23}^2R_{\text{s}} - C_1C_2C_3L_1L_2R_{\text{L}} - C_1C_2C_3L_2L_3R_{\text{s}})),
\end{aligned}
$$

$$
\begin{aligned}
D = {}&(C_1C_2C_3L_2R_{\text{L}}(C_3R_{\text{L}} + C_1R_{\text{s}}) - (C_1C_2L_2 + C_1C_3L_3)(C_1L_1 + C_2L_2 + C_3L_3 + C_1C_3R_{\text{L}}R_{\text{s}}) \\
&+C_1C_3R_L(C_1C_3L_1R_{\text{L}} + C_2C_3L_2R_{\text{L}} + C_1C_2L_2R_{\text{s}} + C_1C_3L_3R_{\text{s}}) - C_1(C_1C_2L_1L_2 - C_1C_3M_{13}^2 \\
&-C_2C_3M_{23}^2 - C_1C_2M_{12}^2 + C_1C_3L_1L_3 + C_2C_3L_2L_3 + C_1C_2C_3L_2R_{\text{L}}R_{\text{s}}) + C_1C_2C_3M_{23}^2 - C_1C_2C_3L_2L_3),
\end{aligned}
$$

$$E = (C_1(C_1L_1 + C_2L_2 + C_3L_3 + C_1C_3R_{\text{L}}R_{\text{s}}) - C_1C_3R_{\text{L}}(C_3R_{\text{L}} + C_1R_{\text{s}}) + C_1C_2L_2 + C_1C_3L_3),$$

$$F = -C_1.$$

The new resonant frequency of the three-coil WPT system can be obtained according to Eq. (11) when the system parameters are changed. Parameters R_1, R_2, and R_3 are set to zero in Eq. (11) because the values of R_1, R_2, and R_3 are small. It can be seen from Eq. (11) that the new resonant frequency of the three-coil WPT system is mainly affected by M_{12}, M_{13}, and M_{23} when the coil parameters are given.

3. THEORETICAL CALCULATION AND SIMULATION VERIFICATION

In this section, the variation law of the new resonant frequency of the three-coil WPT system is studied according to Eq. (11), and the effect of the new resonant frequency on efficiency and output power of the three-coil WPT system is also studied according to Eqs. (6) and (8). These studies provide a theoretical basis for obtaining the optimal efficiency and output power.

3.1. Theoretical Calculation

There exists only pure resistance in the WPT system when the system works in a resonant state. At this time, the efficiency of the WPT system is maximized because most of the power in AC voltage source is transferred to the load. Therefore, the resonant frequencies of the system are also the frequencies

Table 1. Positions with different misalignments and transmission distances.

Position	Distance (cm)				
P_1	$d_1 = 6$	$d_2 = 6$	$\Delta_1 = 0$	$\Delta_2 = 0$	$\Delta_3 = 0$
P_2	$d_1 = 6$	$d_2 = 6$	$\Delta_1 = 6$	$\Delta_2 = 0$	$\Delta_3 = 6$
P_3	$d_1 = 6$	$d_2 = 6$	$\Delta_1 = 12$	$\Delta_2 = 0$	$\Delta_3 = 12$
P_4	$d_1 = 3$	$d_2 = 9$	$\Delta_1 = 0$	$\Delta_2 = 0$	$\Delta_3 = 0$
P_5	$d_1 = 6$	$d_2 = 6$	$\Delta_1 = 10$	$\Delta_2 = 10$	$\Delta_3 = 0$

Table 2. Calculated frequencies corresponding to the maximum efficiency with different positions.

Position	Frequencies (kHz)		
P_1	69.092	73.393	94.272
P_2	\	\	91.611
P_3	\	87.605	\
P_4	66.676	78.112	\
P_5	74.020	77.400	94.694

corresponding to the maximum efficiency. The resonant frequencies are calculated by using Eq. (11). Table 1 shows the positions with different misalignments and transmission distances. Table 2 shows the frequencies corresponding to the maximum efficiency with different positions. Similarly, the frequencies corresponding to the maximum output power are calculated according to Eq. (8). Table 3 shows the frequencies corresponding to the maximum output power with different positions.

Table 2 shows the calculated frequencies corresponding to the maximum efficiency with different positions ('\' denotes that the value does not exist). P_1 is the case when the transmission coil, relay coil, and receiving coil are coaxial. Compared P_1 with other positions, it can be seen that the number of frequency points corresponding to the maximum efficiency is rapidly reduced when the transmission coil is horizontally shifted. The number of frequency points corresponding to the maximum efficiency is slightly reduced when the relay coil is vertically shifted. The number of frequency points corresponding to the maximum efficiency is the same as the case of P_1 when the relay coil is horizontally shifted.

Table 3 shows the calculated frequencies corresponding to the maximum output power with different positions. It can be seen that the number of frequency points corresponding to the maximum output power is slightly reduced when the transmission coil is horizontally shifted, or the relay coil is horizontally shifted. However, the number of frequency points corresponding to the maximum output power is rapidly reduced when the relay coil is vertically shifted. It is concluded that the number of frequency points corresponding to the maximum output power of the system is greatly affected by the vertical shifts of the relay coil.

Table 3. Calculated frequencies corresponding to the maximum output power with different positions.

Position	Frequencies (kHz)		
P_1	68.564	93.504	108.020
P_2	70.108	91.514	\
P_3	72.845	87.631	\
P_4	66.606	\	\
P_5	73.157	94.681	\

There is always a frequency corresponding to the maximum output power which is very close to the frequency corresponding to the maximum efficiency from Table 2 and Table 3. For example, in the case of P_2, there is a maximum efficiency point, and the frequency corresponding to the maximum efficiency point is 91.611 kHz. Similarly, there is a maximum output power point, and the frequency corresponding to the maximum output power point is 91.514 kHz. The difference between the frequency corresponding to the maximum efficiency and the frequency corresponding to the maximum output power is only 0.1%, which provides a theoretical basis for simultaneously obtaining high efficiency and high output power.

3.2. Simulation Verification

In this section, the correctness of the theoretical calculation is verified by the 'mutual inductance' model in MATLAB. The simulated results are shown in Figure 3 till Figure 5.

Figure 3 shows the impedance angle versus ω/ω_0 with different positions. In the case of P_1, there are three resonant frequencies of 69.188 kHz, 73.437 kHz, and 94.344 kHz in the three-coil WPT system. In the case of P_2, there exists a resonant frequency of 91.711 kHz. In the case of P_3, there is a resonant frequency of 87.715 kHz. In the case of P_4, there are two resonant frequencies of 66.765 kHz and 78.196 kHz. In the case of P_5, there are three resonant frequencies of 74.117 kHz, 77.516 kHz, and 94.769 kHz. It can be seen that the number of the resonant frequency points is greatly affected by the position between coils. In most cases, the number of resonant frequency points is reduced with different positions. The difficulty of the system tracking resonant frequency points is increased.

Figure 4 shows the efficiency versus ω/ω_0 with different positions. In the case of P_1, there are four maximum efficiency points. The frequencies corresponding to four maximum efficiency points are 69.188 kHz, 73.437 kHz, 94.344 kHz, and 104.29 kHz, respectively. The efficiencies of four frequency points are 94.19%, 96.33%, 95.32%, and 93.86%, respectively. The impedance angle with the frequency of 104.29 kHz is only 6.74°. Therefore, there exists a high efficiency with this frequency. However, the efficiency with the frequency of 104.29 kHz is still lower than those with resonant frequencies. In
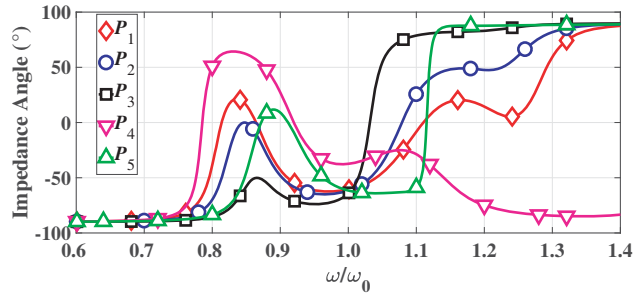
Figure 3. Impedance angle versus ω/ω_0 with different positions.
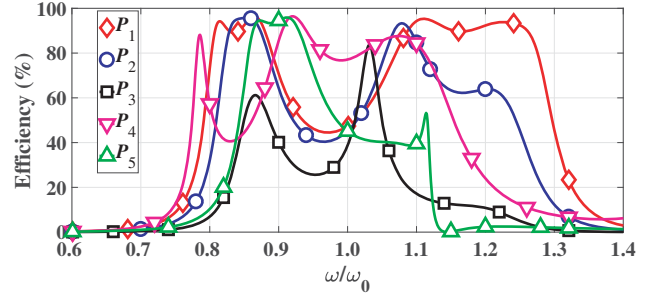
Figure 4. Efficiency versus ω/ω_0 with different positions.
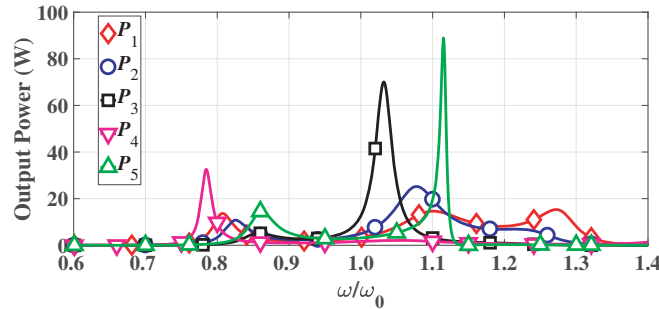
Figure 5. Output power versus ω/ω_0 with different positions.

the case of P_2, there are three maximum efficiency points. The frequencies corresponding to three maximum efficiency points are 72.587 kHz, 91.710 kHz, and 102.33 kHz, respectively. The efficiencies of three frequency points are 95.78%, 93.36%, and 63.9%, respectively. The frequency of 72.587 kHz can be regarded as a resonant frequency because the impedance angle with this frequency is only 0.01°. Therefore, there exists a high efficiency with the frequency of 72.587 kHz. In the case of P_3, there are two maximum efficiency points. The frequencies corresponding to two maximum efficiency points are 73.607 kHz and 87.715 kHz, respectively. The efficiencies of two frequency points are 61.19% and 83.63%, respectively. In the case of P_4, there are three maximum efficiency points. The frequencies corresponding to three maximum efficiency points are 66.808 kHz, 78.196 kHz, and 91.455 kHz, respectively. The efficiencies of three frequency points are 88.15%, 96.45%, and 87.69%, respectively. In the case of P_5, there are three maximum efficiency points, the frequencies corresponding to three maximum efficiency points are 74.202 kHz, 77.516 kHz, and 94.684 kHz, respectively. The efficiencies of three frequency points are 94.53%, 95.91%, and 53.24%, respectively. It can be seen that the frequencies corresponding to the maximum efficiency points of the system are the resonant frequency points. Some frequency points can be considered as quasi-resonant frequency points because impedance angles of these frequency points are nearly equal to zero. Therefore, there is also a high efficiency with quasi-resonant frequency points.

Figure 5 shows the output power versus ω/ω_0 with different positions. The AC input voltage of the WPT system is 12 V. In the case of P_1, there are three maximum output power points. The frequencies corresponding to three maximum output power points are 68.678 kHz, 93.579 kHz, and 108.11 kHz, respectively. The output powers of three frequency points are 13.71 W, 14.64 W, and 15.34 W, respectively. In the case of P_2, there are two maximum output power points. The frequencies corresponding to two maximum output power points are 70.207 kHz and 91.625 kHz, respectively. The output powers of two frequency points are 10.77 W and 25.22 W, respectively. In the case of P_3, there are also two maximum output power points. The frequencies corresponding to two maximum output power points are 72.927 kHz and 87.715 kHz, respectively. The output powers of two frequency points are 5.198 W and 70.07 W, respectively. In the case of P_4, there is only a maximum output power point. The frequency corresponding to the maximum output power point is 66.723 kHz. The output power of this frequency point is 32.56 W. In the case of P_5, there are two maximum output power points. The frequencies corresponding to two maximum output power points are 73.267 kHz and 94.769 kHz, respectively. The output powers of two frequency points are 15.58 W and 88.92 W, respectively. It can be seen that there may be multiple local maximum output powers, including the global maximum output power.

Comparing calculated results with simulated ones, some conclusions can be obtained as follows. First, the frequency corresponding to the maximum efficiency point and the frequency corresponding to the maximum output power point are changed with the change of relative positions. Secondly, the frequency of the maximum efficiency point is nearly the same as the frequency of the maximum power point. In addition, the efficiency and output power with resonant frequency are greatly changed with different positions. There exists a high efficiency but a low output power with some frequencies. On the contrary, there is a high output power but a low efficiency with other frequencies. This is because the frequency corresponding to the maximum power point of the system is not exactly the same as the frequency corresponding to the maximum efficiency point of the system. These two frequencies may be close, but not equal. Some frequencies may be corresponding to the local maximum efficiency, but not corresponding to the global maximum efficiency. Therefore, it is possible that there exists a high output power but a low efficiency with some frequencies. However, for several frequencies, there simultaneously exist high efficiency and output power. Therefore, the frequency selection requires comprehensive consideration of the efficiency and output power.

4. EXPERIMENTAL VERIFICATION

4.1. Experimental Setup

In order to verify the correctness of the theory, a set of experimental devices is designed and developed. The experimental setup is composed of a signal generator, a power amplifier, a digital power meter, a transmission coil, a relay coil, a receiving coil, and a load, as shown in Figure 6. The sine wave signal is generated by the signal generator, which is amplified by a power amplifier. The platform is divided

(a) Experimental setup

(b) Coils
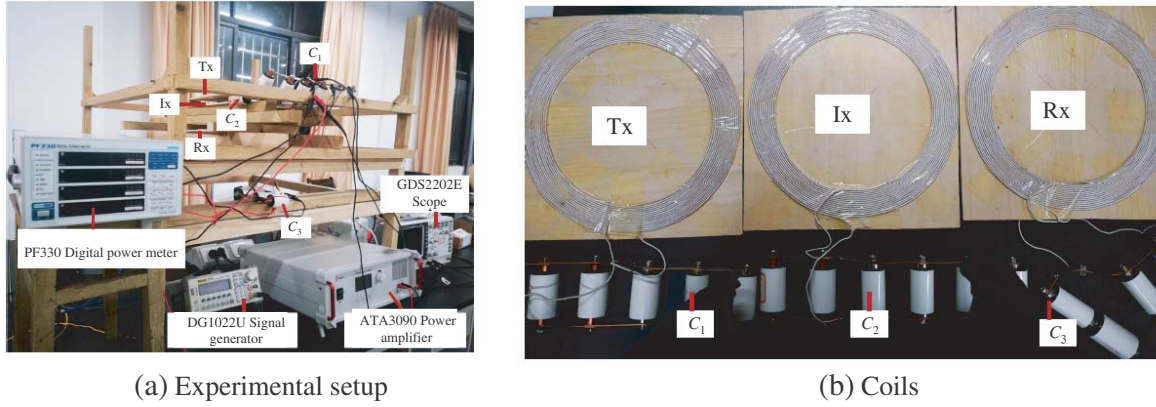
Figure 6. Experimental setup of the three-coil WPT system.

into three layers: the transmission coil is on the top layer, the relay coil on the middle layer, and the receiving coil on the bottom layer. The transmission coil, relay coil, and receiving coil are all composed of planar spiral coils. The inner and outer diameters of the transmission coil, relay coil, and receiving coil are 11.4 cm and 13 cm, respectively. The number of turns of each coil is 15. The coils are made of copper wire with the diameter of 2 mm, as shown in Figure 6(b). The load resistor is a gold resistor with a resistance of 10 Ω. The original resonant frequency of each coil is set to 85 kHz. The resonant frequency, self-inductance (L_i), internal resistance (R_i), and resonant capacitance (C_i) can be obtained with the help of impedance analyzer. Measured parameters of each coil are shown in Table 4.

Table 4. Measured parameters of each coil.

Symbol	Physical meaning	Value
$L_1/\mu H$	The self-inductance of Tx	104.561
$L_2/\mu H$	The self-inductance of Ix	104.245
$L_3/\mu H$	The self-inductance of Rx	105.245
C_1/nF	The resonant capacitance of Tx	33.530
C_2/nF	The resonant capacitance of Ix	33.632
C_3/nF	The resonant capacitance of Rx	33.312
R_1/Ω	The internal resistance of Tx	0.147
R_2/Ω	The internal resistance of Ix	0.151
R_3/Ω	The internal resistance of Rx	0.153

The mutual inductance can be measured with the help of an impedance analyzer. Test method of the mutual inductance is as follows:

(1) The value of L_A can be measured with the help of the impedance analyzer when coil$_1$ is connected to coil$_2$ with the dotted terminal in series. L_1 is the self-inductance of coil$_1$, and L_2 is the self-inductance of coil$_2$. M is the mutual inductance between coil$_1$ and coil$_2$.

(2) The value of L_B can also be measured with the help of the impedance analyzer when coil$_1$ is connected to coil$_2$ with the non-dotted terminal in series. The measured mutual inductance model is shown in Figure 7.

(3) Then, the mutual inductance can be obtained according to $M = (L_A - L_B)/4$.

The measured results of the mutual inductance with different positions are shown in Table 5.
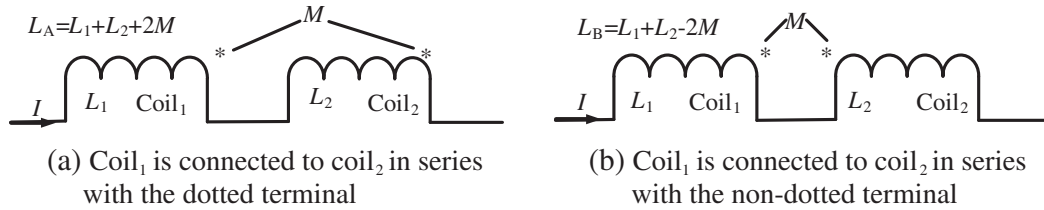
Figure 7. Measured mutual inductance model.

Table 5. Measured mutual inductance with different positions.

Position	Mutual inductance/μH		
	M_{12}	M_{13}	M_{23}
P_1	34.41	16.59	35.38
P_2	27.10	13.76	35.38
P_3	14.62	8.64	35.38
P_4	54.53	16.69	23.73
P_5	20.37	17.53	21.06

4.2. Test of Resonant Frequency

The measured impedance angle curve of the three-coil WPT system can be measured by the impedance analyzer. The data of the impedance angle can be plotted by EXCEL as shown in Figure 8. It is clearly seen that the measured impedance angle is basically the same as the simulated impedance angle. The correctness of the simulation results is verified. From Figure 8, the resonant frequency of the WPT system is changed, and the number of the resonant frequency points is reduced with different positions. Therefore, the resonant frequency of the WPT system is greatly affected by different positions.
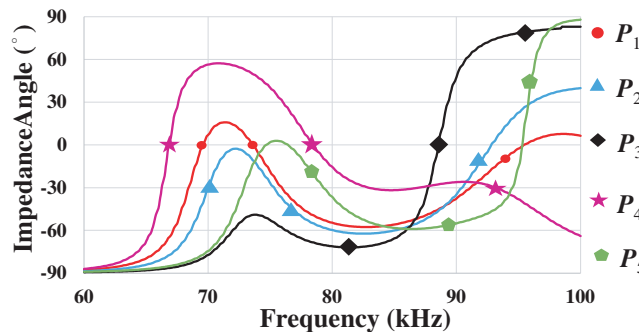
Figure 8. Measured impedance angle versus frequency with different positions.

The resonant frequencies with different positions can be measured with the help of the impedance analyzer, as shown in Table 6. It is clearly seen that the errors between experimental and simulated results are less than 1.2%. The correctness of the resonant frequency calculation method is verified. From P_1 to P_3, the number of the resonant frequency points is rapidly reduced when the relay coil and receiving coil are coaxial, and the transmission coil is horizontally shifted. Comparing P_4 with P_1, the number of the resonant frequency points and the values of resonant frequency are smoothly changed when the transmission coil, relay coil, and receiving coil are coaxial, and the relay coil is vertically shifted. Comparing P_5 with P_1, the number of resonant frequency points and the values of resonant frequency are slightly changed. It means that the resonant frequencies of the system are less affected

Table 6. Measured resonant frequencies with different positions.

Position	Frequencies (kHz)		
P_1	69.6	73.6	94.8
P_2	\	\	92.8
P_3	\	88.6	\
P_4	66.8	78.5	\
P_5	74.6	76.6	94.3

in the case of P_5. As can be seen from Table 6, the effect of the horizontal shift of the coils on the resonant frequency is more than that of the vertical shift of the coils on the resonant frequency.

The frequencies corresponding to the maximum output power with different positions are measured by digital power meter, as shown in Table 7. The output voltages are maximum at the frequency points in Table 7. It is clearly seen that the errors between the measured and simulated results are less than 2.5%. The correctness of the frequency calculation method corresponding to the maximum output power is verified. It is helpful for obtaining the maximum output power point in the three-coil WPT system according to Eq. (8).

Table 7. Measured frequencies corresponding to the maximum output power with different positions.

Position	Frequencies (kHz)		
P_1	68.5	92.5	106.5
P_2	71.0	90.5	\
P_3	73.5	86.5	\
P_4	66.5	\	\
P_5	73.0	94.0	\

5. CONCLUSION

In this paper, the frequency characteristics, transmission efficiency, and output power of the three-coil WPT system are analyzed in detail with different positions. The expressions of the resonant frequency and maximum output power are deduced with different positions. Based on these expressions, the frequencies corresponding to the maximum efficiency and the frequencies corresponding to the maximum output power are calculated. A set of experimental devices is developed, and the measured results are consistent with the calculated and simulated ones, which verifies the correctness of the proposed method.

The resonant frequency, efficiency, and output power in the three-coil WPT system are changed when the relative positions are changed. The efficiency of the WPT system can be maximized when the system works in a resonant state. The system always features a maximum efficiency point and a maximum output power point. The frequencies of the two points are almost the same. When the vertical distance is constant and Δ_1 gradually increased, the number of resonant frequency points is gradually decreased. And the number of maximum output power points and the number of maximum efficiencies are decreased at the same time. In addition, the efficiencies with the resonant frequency points are decreased dramatically with the increase in Δ_1. However, the output powers with the resonant frequency points are increased. Therefore, the frequency selection requires comprehensive consideration of the efficiency and the output power according to practical applications. When the horizontal distance is constant but d_1 and d_2 are changed, the number of resonant frequency points is decreased, and the efficiency of the WPT system is reduced. Therefore, a proper vertical distance is important for obtaining high efficiency.

These theories provide a feasible scheme for simultaneously achieving high efficiency and output power and also provide a useful reference for the further research on the frequency tracking and optimization control algorithms.

ACKNOWLEDGMENT

REFERENCES

1. Liu, Z. and Z. Z. Chen, "A magnetic tank system for wireless power transfer," *IEEE Trans. Power Electron.*, Vol. 27, No. 5, 443–445, May 2017.
2. Liu, C. and C. Jiang, "An effective sandwiched wireless power transfer system for charging implantable cardiac pacemaker," *IEEE Trans. Ind. Electron.*, Vol. 66, No. 5, 4108–4117, May 2019.
3. Mi, C. C. and S. Y. Choi, "Modern advances in wireless power transfer systems for roadway powered electric vehicles," *IEEE Trans. Ind. Electron.*, Vol. 63, No. 10, 6533–6545, Oct. 2016.
4. Li, Z. and C. Zhu, "A 3-kW wireless power transfer system for sightseeing car super capacitor charge," *IEEE Trans. Power Electron.*, Vol. 32, No. 5, 3301–3316, May 2017.
5. Kurs, A., A. Karalis, R. Moffatt, J. D. Joannopoulos, P. Fisher, M. Soljačić, "Wireless power transfer via strongly coupled magnetic resonances," *Science*, Vol. 317, No. 6, 83–86, Jul. 2007.
6. Zhang, Z. and H. Pang, "Wireless power transfer — An overview," *IEEE Trans. Ind. Electron.*, Vol. 66, No. 2, 1044–1058, Feb. 2019.
7. Fu, M. and H. Yin, "A 6.78 MHz multiple-receiver wireless power transfer system with constant output voltage and optimum efficiency," *IEEE Trans. Power Electron.*, Vol. 33, No. 6, 5330–5340, Jun. 2018.
8. Kan, T. and F. Lu, "Integrated coil design for EV wireless charging systems using LCC compensation topology," *IEEE Trans. Power Electron.*, Vol. 33, No. 11, 9231–9241, Nov. 2018.
9. Hu, H. and S. V. Georgakopoulos, "Multiband and broadband wireless power transfer systems using the conformal strongly coupled magnetic resonance method," *IEEE Trans. Ind. Electron.*, Vol. 64, No. 5, 3595–3607, May 2017.
10. Che, W. and Q. Wang, "Wireless power transfer with three-ports networks: Optimal analytical solutions," *IEEE Trans. Circuits Syst. I, Reg. Papers*, Vol. 64, No. 2, 494–503, Feb. 2017.
11. Rozman, M., et al, "Combined conformal strongly-coupled magnetic resonance for efficient wireless power transfer," *Energies*, Vol. 10, No. 4, 498–515, Apr. 2017.
12. Zhang, Z. and K. T. Chau, "Energy encryption for wireless power transfer," *IEEE Trans. Power Electron.*, Vol. 30, No. 9, 5237–5246, Sept. 2015.
13. Mastri, F. and A. Costanzo, "Coupling-independent wireless power transfer," *IEEE Microw. Wireless Compon. Lett.*, Vol. 26, No. 3, 222–224, Mar. 2016.
14. Hui, S. Y. R. and W. Zhong, "A critical review of recent progress in mid-range wireless power transfer," *IEEE Trans. Power Electron.*, Vol. 29, No. 9, 4500–4511, Sept. 2014.
15. Sample, A. P. and D. A. Meyer, "Analysis, experimental results, and range adaptation of magnetically coupled resonators for wireless power transfer," *IEEE Trans. Ind. Electron.*, Vol. 58, No. 2, 544–554, Feb. 2011.
16. Zhang, Y. and Z. Zhao, "Frequency-splitting analysis of four coil resonant wireless power transfer," *IEEE Trans. Ind. Appl.*, Vol. 50, No. 4, 2436–2445, Jul. 2014.

17. Zhang, Y. and L. Ting, "Selective wireless power transfer to multiple loads using receivers of different resonant frequencies," *IEEE Trans. Power Electron.*, Vol. 30, No. 11, 6001–6005, Aug. 2015.

18. Ahn, D., "Transmitter coil resonant frequency selection for wireless power transfer," *IEEE Trans. Power Electron.*, Vol. 33, No. 6, 5029–5041, Jul. 2018.

19. Lee, J. and K. Lee, "Stability improvement of transmission efficiency based on a relay resonator in a wireless power transfer system," *IEEE Trans. Power Electron.*, Vol. 32, No. 5, 3297–3300, Jul. 2011.

20. Kiani, M. and U. Jow, "Design and optimization of a 3-coil inductive link for efficient wireless power transmission," *IEEE Trans. Biomed. Circuits Syst.*, Vol. 5, No. 6, 579–591, May 2017.

21. Zhang, J. and C. Cheng, "Analysis and optimization of three-resonator wireless power transfer system for predetermined-goals wireless power transmission," *Energies*, Vol. 9, No. 4, 274–293, Apr. 2016.

22. Sun, L. and H. Tang, "Determining the frequency for load independent output current in three-coil wireless power transfer system," *Energies*, Vol. 8, No. 9, 9719–9730, Sept. 2015.